



## SOURCE PARAMETERS FROM ACCELERATION RECORDS FOR EARTHQUAKES FROM 1987-2008 IN SOUTH ICELAND

S. Ólafsson<sup>(1)</sup>, R. Rupakhety<sup>(2)</sup>.

<sup>(1)</sup> Research Professor, Earthquake Engineering Research Centre, University of Iceland, [simon@hi.is](mailto:simon@hi.is)

<sup>(2)</sup> Associate Professor, Earthquake Engineering Research Centre, University of Iceland, [rajesh@hi.is](mailto:rajesh@hi.is)

...

### **Abstract**

In the year 2000 two earthquakes struck South-Iceland (17 June -  $M_w$  6.5; 21 June -  $M_w$  6.4). These were the largest earthquakes in South-Iceland since 1912 ( $M7$ ) and were recorded on 25 strong motion stations. In 2008 a third earthquake,  $M_w$  6.3, struck with an epicentre only 30 km west of the fault 21 June 2000 event and was also recorded on several strong motion stations. In this article the source parameters using Brune's extended source model are computed for these earthquakes using the ground acceleration records. A frequency independent  $Q$  is assumed and kappa ( $\kappa$ ) is estimated. The corner frequency and seismic moment are also estimated. These parameters that can be obtained from the strong-motion acceleration records along with a duration and a geometric attenuation function can provide a model that gives a good fit to measured the ground motion. The largest earthquakes in South Iceland have a right lateral strike-slip mechanism. They occur on parallel N-S trending faults with near vertical fault planes and their focus is shallow and extends all the way to the earths surface. Comparatively high acceleration values with regard to the size of the faults are observed in the source region and there is a rapid attenuation of in the near- and inter-mediate field This effect is demonstrated and a point source model with a geometric attenuation function is demonstrated to provide a good representation of strong-motion acceleration recorded in the earthquakes using the estimated parameters.

*Keywords: Source parameters, kappa, stress drop, geometric attenuation, peak factor*

### **1. Introduction**

This article focuses on five of the largest earthquakes that have occurred in South Iceland from 1912-2008 with magnitudes that range from  $M$  6 to  $M$  7. In four of these earthquakes strong-motion records were obtained and they are important for seismic hazard assessment. The fifth earthquake is the 1912  $M_S$  7 event and is important because it represents what is believed to be the largest earthquakes that can be expected to occur in the region. It is therefore very important to consider that event in seismic hazard assessment. The lack of strong-motion records from events of that magnitude and characteristics that are specific to the region provides for a challenging problem for estimation of design ground motions.

The article will focus on estimating the parameters (kappa, seismic moment and stress drop) of a point source model (Brune 1970 [1]), extended with an exponential term to account for high frequency decay, using strong-motion records obtained in four earthquakes. This is a simple ground motion model that can in most cases give an adequate description for engineering purposes and probabilistic studies. A properly extended and calibrated point source model can in fact be used instead of empirical ground motion models to "predict" the necessary design ground motions. Ground motions considered as bandlimited white noise with spectral characteristics defined by Brune's model has been shown to be in good agreement with recorded ground motions



(see Hank and McGuire 1981 [2]; Boore 1983; Atkinson and Boore, 1995 [3]; Ólafsson and Sigbjörnsson, 1999 [4]).

The Brune model was first applied to Icelandic strong motion data by Ólafsson and Sigbjörnsson [4] and used to construct a GMPE for Iceland. The main reasons for using this approach was the lack of data to provide reliable empirical GMPE's. At that time the largest earthquake that strong-motion acceleration with strong-motion acceleration records was the Vatnafjalla earthquake ( $M_w$  5.8) and the model was calibrated based on parameters estimated for that earthquakes (see Ólafsson et a. 1998 [5]; Ólafsson, 1999 [6]). Since then three larger earthquakes have occurred in the area, two events in 2000 ( $M_w$  6.5 and  $M_w$  6.4) and an  $M_w$  6.3 event in 2008. These events have provided valuable strong-motion records that have been obtained from the various stations in the Icelandic Strong Motion Network (IceSMN) [7]. An attenuation relationship based on a point source model (Ólafsson and Sigbjörnsson [4], [8], [9]) has been used in many hazard assessments in Iceland (see for example [10]). The parameters for the 2000 and 2008 earthquakes have been reported as part of earlier articles but have not been presented properly in conference proceedings or journal articles. The main incentive for using a point source model were the lack of data to develop empirical relations and also the regional characteristics that were observed; relatively short duration and high acceleration values.

The IceSMN was initiated in 1985 with the installation of 6 Geotech A700 recorders. The network has been in operation since then in the most seismically active zones in North- and South-Iceland and has experienced healthy growth. In addition to ground response, there are many stations (such as bridges, high-rise buildings, power-plants, and dams) where structural response is monitored in addition to ground response. Records from earthquakes can be found in the Internet Site for European Strong Motion Data [11]. The Centre is located in Selfoss in the SISZ and was founded in 2000 by Professor Ragnar Sigbjörnsson. Before that time the network was operated by the Applied Mechanics Laboratory of the University of Iceland. Operating the IceSMN has been vital for the Earthquake Engineering Research Centre of the University of Iceland and the strong-motion records obtained by the network have been very important in earthquake engineering research in Iceland.

## 2. South Iceland Seismic Zone and recorded strong-motion earthquakes

The South Iceland Seismic Zone (SISZ) shown in Fig. 1 is part of the Mid-Atlantic ridge and is located in the lowland between Hellisheiði (and Hengill volcano) in the West and Mount Hekla, 80 km further east. The SISZ is an east-west left lateral transform zone between the two continental plates, merging into the American plate to the North and the Eurasian plate to the south. The largest earthquakes in the SISZ occur on N-S trending faults that are perpendicular to the left-lateral E-W movements of the two continental plates. The term bookshelf tectonics is used to describe this type of mechanics [12]. The earthquakes occur on north-south trending right lateral strike-slip faults with near vertical fault planes at shallow depths. The rupture reaches the surface for the largest earthquakes where the whole seismogenic zone ruptures down to the bottom of the crust. In the two volcanic zones to the east and west of the SISZ the earthquakes are typically smaller with a different source mechanism (normal). From information about historical events and some instrumentally recorded larger events, it has been observed that the earthquakes in this area can reach a magnitude of approximately 7 (Ambraseys and Sigbjörnsson [13]). The earthquakes occur in sequences with a return period of 45-110 year. The largest earthquakes occur in the eastern part of the SISZ. Typically the sequence of earthquakes starts in the east and migrates to the west (Einarsson [12]). In North-Iceland, there is a similar transform zone but, unlike the SISZ, which is or located in populated agricultural area, the TFZ is located off shore.

The fault traces of the most recent major earthquakes in the SISZ are shown in Fig. 1. Also shown are the stations in the IceSMN, indicated by black triangles. The fault traces represent four major earthquakes (6 May 1912 -  $M_s$  7; 17 June 2000 -  $M_w$  6.5; 21 June 2000 -  $M_w$  6.4; and 29 May 2008 -  $M_w$  6.3). The fault trace furthest to the east, represents the earthquakes on May 6<sup>th</sup> 1912 [13], [14]. The other three earthquakes all occurred after the initiation of IceSMN in 1985. A brief description of each earthquake follows (see also Table 1 for basic information about the earthquakes).

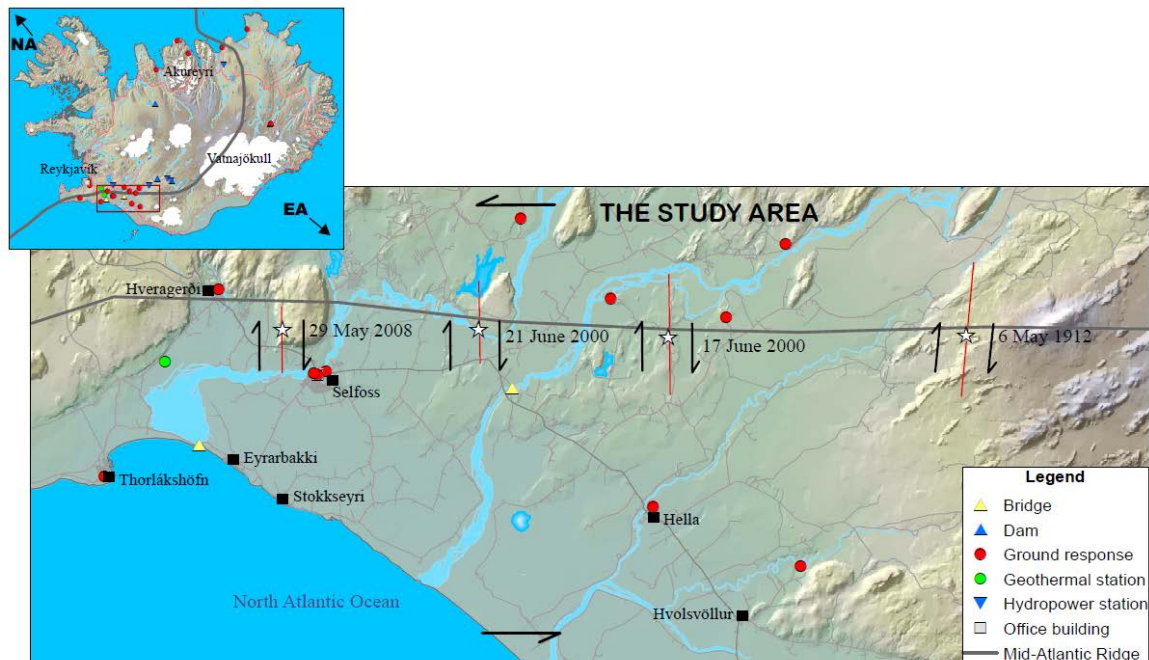


Fig. 1 – The South Iceland Seismic Zone and its seismo-tectonics. The small arrows at the top and bottom of the main image show the left-lateral transform motion of the zone. Inset map shows relative motion across the boundary of the two continental plates. Faults traces are shown of major earthquakes in the area during the period 1912-2008 (6 May 1912 -  $M_s$  7; 17 June 2000 -  $M_w$  6.5; 21 June 2000 -  $M_w$  6.4; and 29 May 2008 -  $M_w$  6.3). Stations in the IceSMN are shown as symbols described in the legend.

#### Vatnafjoll earthquake 25 May 1987 11:32 $M_w$ 5.8

The fault trace of this earthquake is not shown in Fig. 1 but is located on the boundary of the SISZ and the eastern volcanic zone. This was the largest earthquake in this area since the 1912  $M$  7 earthquake. This was also the first earthquake that was recorded by the newly established IceSMN. The fault did not reach the surface.

#### Rangárvellir 6 May 1912 18:59 $M_s$ 7

The 1912 Rangárvellir earthquakes  $M_s$  7 was the last earthquake in a sequence of earthquakes that included events in 1886. Examining surface faults Bjarnason et al. 1993 [14] estimated that the earthquake ruptured on a fault plane 20 km long and 15 km deep with an average slip of 2.4-3.3m.

#### Holt, 17 June 2000 14:51 $M_w$ 6.5

On June 17, 2000 at 15:40, an earthquake struck in South-Iceland, just north of the town of Hella (see Fig.1) in an area called Holt at a depth of 6 km. The highest PGA measured was 64% in the basement in Kaldarholt (Station 103). In South Iceland there was considerable structural damage but no casualties.

#### Hestfjall, 21 June 2000 00:51 $M_w$ 6.4

Just after midnight only four days later, another earthquake struck in the center of the SISZ on a fault 17 km west of the June 17<sup>th</sup> at a depth of 5 km. The highest PGA measured was approximately 84% g on the west pillar of the Thjórsá River Bridge (Station 502).

#### Ölfus 29 May 2008 15:45 $M_w$ 6.3

The earthquake was originated on faults only 2 km east of the town of Hveragerði. The earthquake occurred on two faults, with the second fault located 4 km west of the first fault. In addition to the strong-motion records obtained in the IceSMN network the earthquake was measured on a recently installed strong-motion array in



Hveragerði called ICEARRAY. Those measurements are not included in this study except for information of mean and highest values of PGA. Records were obtained from eleven ICEARRAY stations with Joyner-Boore distances in the range of 0.9 to 2.3 km with a largest horizontal PGA of 0.86g and mean PGA of 0.61g (see Halldórsson and Sigbjörnsson, 2009 [15]).

Table 1 – The five largest earthquakes in South Iceland from 1912-2008. PGA values for horizontal and vertical acceleration are shown. No strong-motion measurements were made before 1985.

Earthquake	Date - Time	Magnitudes	Epicentre		IceSMN stations	Acceleration	
			°W	°N		Horizontal PGA(g)	Vertical PGA(g)
Rangárvellir	06.05.1912 18:59	$M_s$ 7.0	19.83	63.98	-		
Vatnafjöll	25.05.1987 11:32	$M_w$ 5.8	21.19	64.00	7	0.06	0.05
South-Iceland, Holt	17.06.2000 15:41	$M_w$ 6.5	20.36	63.97	25	0.61	0.63
South-Iceland, Hestfjall	21.06.2000 00:51	$M_w$ 6.4	20.71	63.98	24	0.83	0.54
Ölfus	29.05.2008 15:45	$M_w$ 6.3	21.01	64.10	8	0.86	0.82

A characteristic of the strong-motion records obtained from these earthquakes are the comparatively high acceleration values close to the fault. To demonstrate this, the PGA values of horizontal acceleration recorded in the 21 June 2000 earthquake are plotted in Fig. 2 with attenuation curves from the model of Akkar et al. (2014) [16]. The PGA values are plotted as a function of two distance measures with red-triangles representing epicentral distances and black circular dots representing Joyner-Boore distances. The Akkar et al. model [16] is also plotted for two distance measures, with the black-solid line representing the Joyner-Boore distance and the red-dotted line representing epicentral distance. From Fig. 2 it can be observed that the GMPE model gives values that are too low for the ground motion at short distances from the fault and gives values that are too high at larger distances. The Akkar et al. model was also tested for hypocentral distance with similar results.

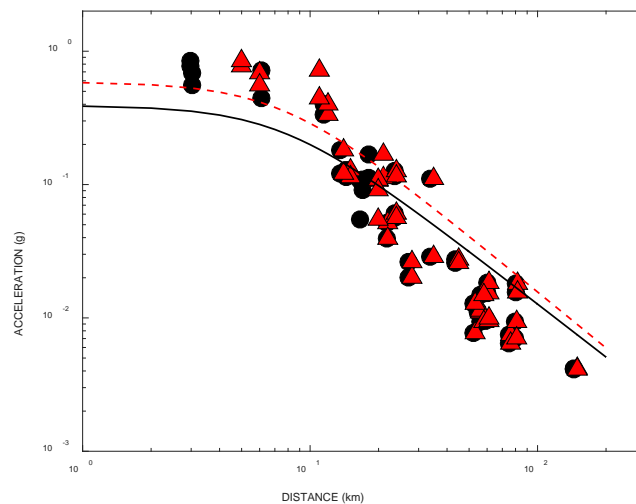


Fig. 2 – Horizontal PGA values from strong-motion records obtained in the earthquakes of 21.06.2016 plotted as a function of epicentral distance (triangles) and Joyner-Boore distance (circles). Attenuation model of Akkar et al. [16] is plotted for epicentral distance (red dashed line) and Joyner-Boore distance (black solid).



Underprediction of the ground motion, for the Icelandic earthquakes, at short distances is typical for the empirical GMPE's found in the literature. It is very important when performing probabilistic hazard assessment for the area, that a ground motion model be used that gives a realistic representation of the near-field ground motion, where most of the damage usually occurs. In this article it is demonstrated that a point source model using a geometrical attenuation function gives a fair representation of the data obtained from the four largest earthquakes that have been recorded in Iceland by the strong-motion network to date.

The ground motion recorder sites are either classified as rock or stiff soil, so the site response is neglected in the work presented in this paper.

### 3. Applied models and methods

The method applied is to select the S-wave portion of the accelerograms that contains most of the energy at epicentral distances less than 100 km. Then parameters  $\kappa$ ,  $\omega_c$  and  $M_0$  are estimated by fitting spectra obtained from the S-wave window portion of the acceleration records to Brune's model [1] that has been extended with an exponential term to account for high-frequency decay. The far-field model of Brune is defined as follows, in Eq. 1, as a displacement amplitude spectrum

$$|D(\omega)| = \frac{2C_p R_{0\phi} M_0}{4\pi\beta^3\rho R} \frac{1}{(1 + (\omega/\omega_c)^2)} \exp(-\frac{1}{2}\kappa\omega) \quad (1)$$

Here  $C_p = 0.707$  is the factor that accounts for the partition of the energy between the components,  $R_{0\phi}$  is the S-wave radiation pattern (average is 0.55),  $\beta$  is the shear wave velocity, and  $\rho$  is the density of the crust. Anderson and Hough (1984) [17] found it was possible to describe strong-motion acceleration with a frequency independent  $Q$  in shallow crust and a spectral decay parameter of  $\kappa=R/Q\beta$ . Here  $\omega_c$  is the corner frequency as defined as (Brune, 1970)  $f_c = \omega_c/2\pi$ . The radius of the dislocation, where  $r$  is related to the corner frequency as follows according to Brune:

$$r = 2.34 \cdot \beta / \omega_c \quad (2)$$

The stress drop,  $\Delta\sigma$ , is given as follows

$$\Delta\sigma = \frac{(7/16)M_0}{r^3} \quad (3)$$

This is found as a reasonable approximation for the study area, at least for moderate-sized earthquakes (Ólafsson et al. 1998 [5]). The average displacement of the fault is

$$u = \frac{M_0}{\mu A} \quad (4)$$

$A$  is the area of the fault and  $\mu$  is rigidity given as  $\mu = \rho\beta^2$ . The high frequency attenuation is controlled by the parameter  $\kappa$ , which is assumed to be distance independent (see Anderson and Hough [17]) and a frequency independent  $Q$  that changes linearly with distance from the source. The distance term in equation is represented by  $R$  and it is a function of the hypocentral distance,  $D$ .

$$D = \sqrt{d^2 + h^2} \quad (5)$$



The term  $d$  is the epicentral distance and  $h$  is the depth parameter. Close to the fault  $R \sim D^2$ , at least for strong motion earthquakes and further away from the fault  $R = D$ . The estimation of the three parameters is a two stage process (see Ólafsson et al. 1998 [5] and Ólafsson, 1999 [6]). After selecting the S-wave window from the strong-motion records the acceleration amplitude spectra are obtained from those records and are dominated by the exponential term  $e^{-\omega R/2Q\beta}$  at high frequencies. The values for  $Q$  were obtained by fitting a regression line to the acceleration spectra from 2 to 25 Hz. The amplitude spectra,  $A(\omega) = \omega^2 D(\omega)$ , are dominated by the exponential term at high frequencies. Having determined  $Q$  then  $\kappa$ , is obtained as

$$\kappa = \frac{R}{Q\beta} \quad (6)$$

For the estimation of the corner frequency and the seismic moment the Fourier displacement spectra is obtained from the strong-motion records and the model in Eq. (1) fitted using non-linear optimization. Usually the displacement spectra  $D(\omega)$  is obtained by dividing the acceleration spectra  $A(\omega)$  with  $\omega^2$ ,  $D(\omega) = A(\omega)/\omega^2$ . Before the optimization is performed the exponential term is removed by dividing by  $e^{-\omega R/2Q\beta}$  to obtain the spectra at the source. It is also necessary to take into account if there is a geometric attenuation relationship applied, resulting in a distance range where at some segments where  $R \sim D^n$  and  $n=1$  does not apply. For the largest Iceleandic earthquakes we have found that close to the fault  $n = 2$ . We do not have enough data to determine  $n$  for distances larger than 100 km, where typically  $n = 0.5$  to account for surface waves.

An alternative method for determining the source parameters, seismic moment and corner frequency, is using the spectral moment method (see Andrew, 1986 [18]). This method is also applied here, in addition to the non-linear optimization, and found in many cases, to give estimates with lower standard deviations.

## 4. Estimated parameters

### 4.1 Estimation of kappa.

Estimates of the parameter  $\kappa$  were obtained for all the strong-motion records of the four more recent earthquakes listed in Table 1. The following values were used for all earthquakes: S-wave velocity and density,  $\beta = 3.5$  km/s and  $\rho = 2.8$  g/cm<sup>3</sup>. The resulting  $\kappa$  values are plotted in Fig. 3 for each earthquake as function of distance from the fault. A regression line is included to determine the two regression parameters,  $\kappa_0$  (an intercept with the vertical axis) and  $c$  (measures rate of increase in  $\kappa$  with distance):

$$\kappa = \kappa_0 + cD \quad (7)$$

Kappa is seen to vary slowly with respect to distance as Anderson and Hough (1984) [17] found for California earthquakes. Table 2 shows similar results can be seen for all the earthquakes, and the average kappa is  $\kappa = 0.045$  s. It can be said that  $\kappa = \kappa_0$  is approximately valid for distances less than 100 km.



Table 2 – Parameters for Eq. (7).  $\kappa_0$  and  $c$  and then the average value of  $\kappa$  from all the station recorded in the four earthquakes.

Earthquake	Date	Time	$\kappa_0$ (s)	$c$	$\kappa$ (s)
Vatnafjöll	25.05.1987	11:31	0.0417	0.0001	0.044
South-Iceland, Holt	17.06.2000	15:41	0.0428	0.0002	0.043
South-Iceland, Hestfjall	21.06.2000	00:51	0.0347	0.0002	0.045
Ölfus	29.05.2008	15:45	0.0434	0.0001	0.046

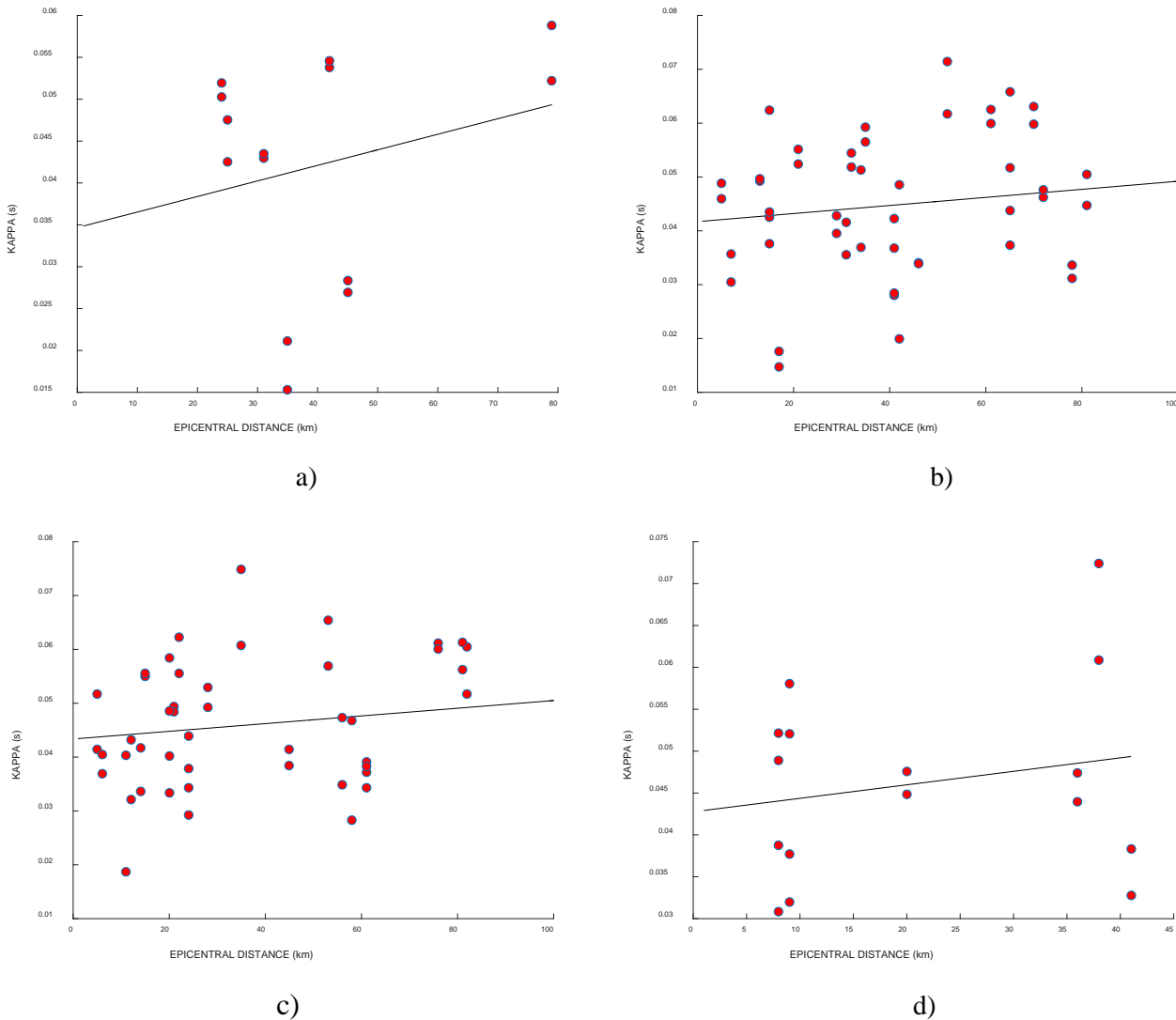


Fig.3 – Spectral decay parameter,  $\kappa$ , as a function of distance and a regression line as described in Eq. (7). a) 25 May 1987. b) 17 June 2000. c) 21 June 2000. d) 29 May 2008.



#### 4.2 Results of estimates of $\omega_c$ and $M_0$ .

The parameters  $\omega_c$  and  $M_0$  are estimated by fitting the Brune displacement spectrum (Eq. (1)) with the two methods described in section 3. The average results are shown in Table 3. The derived quantities i.e. radius of fault  $r$  (Eq. (2)), stress drop,  $\Delta\sigma$ . (Eq. (3)) and average dislocation,  $u$ , given by Eq. (4) are also shown. Fig. 4 shows the model in Eq. (1) that has been fitted to a displacement spectrum with good results. Unfortunately the model does not fit as well for all the records and the worst cases were, therefore omitted when the average parameters were computed. The standard deviation of the parameters, which was large, was examined for both methods. The results with the lowest standard deviation was chosen. It should be mentioned that computing the average values of the corner frequencies for all the stations and then computing the derived parameters  $r$ ,  $\Delta\sigma$  and  $u$ , did not give realistic values. The alternative method was used to compute  $r$ ,  $\Delta\sigma$  and  $u$  for each station and then obtain an average of those values.

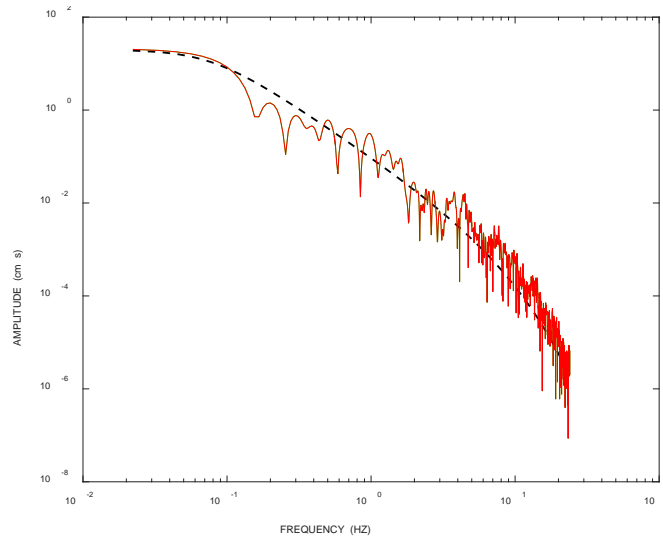


Fig. 4 – Brune's point source model, Eq. (1), represented by the black dashed line, fitted to the displacements amplitude spectrum (red line) computed from the S-wave window of a strong-motion record from the Thorlakshofn station in the 17 June 2000 earthquake.

Table 3 – Source parameters for the four earthquakes. (For  $\Delta\sigma$ : 1bar =  $10^5$  Pa). (For  $M_0$ : 1dyn-cm =  $10^{-7}$ N-m). The parameters are: stress drop  $\Delta\sigma$ , fault radius  $r$ , dislocation of fault  $u$ , seismic moment  $M_0$ .

Earthquake	Date	Time	$f_c$ (Hz)	$\Delta\sigma$ (bar)	$r$ (km)	$u$ (cm)	Fault area (km <sup>2</sup> )	$M_0$ dyn-cm	$M_w$
Vatnafjöll	25.05.1987	11:31	0.36	48	3.6	33	41	$5.3 \times 10^{24}$	5.78
South-Iceland, Holt	17.06.2000	15:41	0.20	80	6.6	89	137	$53 \times 10^{24}$	6.45
South-Iceland, Hestfjall	21.06.2000	00:51	0.22	83	6.0	78	113	$41 \times 10^{24}$	6.37
Ölfus	29.05.2008	15:45	0.24	82	5.4	94	92	$30 \times 10^{24}$	6.27

## 5. Estimate of rms-acceleration and PGA

### 5.1 Simulation with stochastic method

Using Parsevals theorem the following equations can be obtained by using Brune's model in Eq. (1) (see Ólafsson, 1999; Ólafsson and Sigbjörnsson, 1999). Here  $\Psi$  is a function of  $\lambda = \kappa\omega_c$  and the solution is in terms of



sine and cosine integrals. It is also possible to get a good approximation of  $\Psi$  using an exponential function with two parameters as in Eq. (10). Duration is also a parameter that needs to be estimated. The duration used is the 90% of the cumulative energy duration and can be approximated by a function such as in Eq. (11). A plot of the duration function appears in Fig. 5. Also plotted in the graph is the selected duration of the S-wave window used for determining the source parameters (green dots). The parameters of the duration equation, Eq. (11), are dependent on the size of the earthquake, and they are  $[c_1 \ c_2 \ c_3]$ . The standard deviation  $\sigma_T$  is not considered here. The parameters for a magnitude  $M \ 6.5 \pm 0.2$  is;  $[1.50 \ 0.10 \ 1.20]$  and for  $M \ 6 \pm 0.2$   $[2.00 \ 0.05 \ 1.17]$ . The  $a_{rms}$  values were estimated using Eqs. (8), (9), (10), (11), (12) and the plotted against the values of  $a_{rms}$  obtained directly from the S-wave time window. It should be mentioned that the geometric attenuation was proportional to  $D^{-2}$  for distances less than 20 km for the  $M_w \ 6$  earthquakes but the same for the other ( $M_w \ 6.3$ ,  $M_w \ 6.4$  and  $M_w \ 6.5$ ) earthquakes for distances less than 30 km from the source. Equation 8 gives Brune relationship between  $\omega_c$  and stress drop  $\Delta\sigma$  and seismic moment  $M_0$ . It should be noted that the equations are set up for using cm for distance and dyne cm for seismic moment,  $M_0$ . Therefore PGA will be in  $\text{cm/s}^2$ . The factor  $p$  is the peak factor, which is found to be close to 3.2 on average for the earthquakes studied here. Using  $p = 3$  is good approximation in most cases.

$$\omega_c = 2.34(16/7)^{1/3} \beta \left\{ \frac{\Delta\sigma}{M_0} \right\}^{1/3} \quad (8)$$

$$a_{rms} = \frac{0.57 \cdot \Delta\sigma^{2/3} \Psi^{1/2} M_0^{1/3}}{\beta \rho \sqrt{\kappa T_d} R} \quad (9)$$

$$\Psi = \exp(-1.5(\kappa\omega_c)^{0.87}) \quad (10)$$

$$T_d = c_1 \frac{r}{\beta} + c_2 d^{c_3} + \sigma_T \quad (11)$$

$$PGA = p \cdot a_{rms} \quad (12)$$

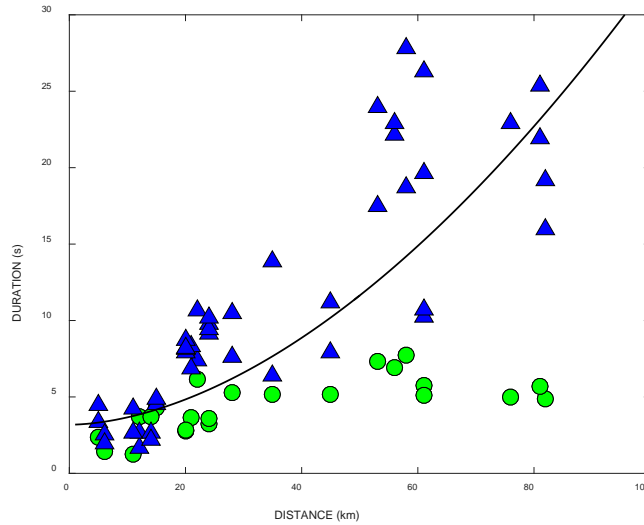


Fig. 5 – Duration for the 21.07.2000 event. Blue triangles are duration values at each station based on 90% of cumulative energy. The green dots represent the chosen S-wave window duration. The line represents the model of Eq. (11) with parameters.

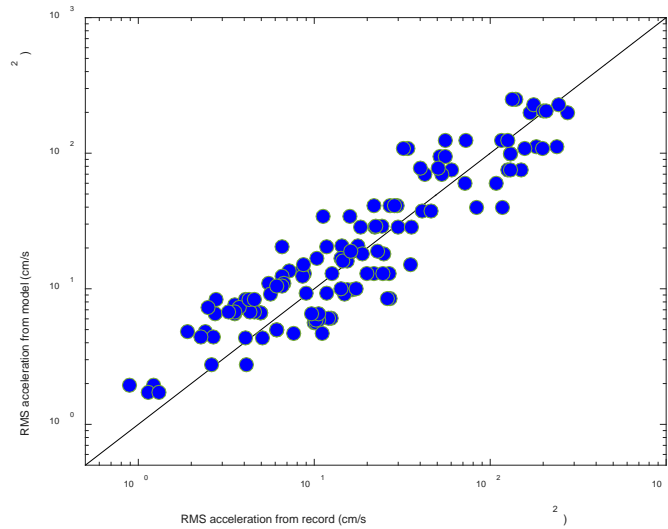


Fig. 6 – Rms-acceleration from acceleration records and by simulation compared for all 4 earthquakes.

Fig. 7 shows the simulated PGA values for the 21 June 2000 earthquake using Eqs. (9) – (12), using the parameters of Eq. (1) in Table 3. In parenthesis the unit used in Eq. (9) for S-wave velocity:  $\beta = 3.5$  km/s (cm/s), Density of the crust:  $\rho = 2.8$  g/cm<sup>3</sup> (g/cm<sup>3</sup>), Stress drop: 83 bar (dyne/cm<sup>2</sup>), Seismic moment;  $M_0 = 41 \times 10^{24}$  dyne cm (dyne cm) are shown. The parameter for the duration function in Eq. (11) that were recommende for an  $M_w$  6.5 earthquake were used (note that the epicentral distance  $d$  should have units of km in that equation). Fig. 7 shows the PGA values of horizontal acceleration (both components) for the earthquake of 21.06.2000 as represented by red dots in both Figs. 7 a) and b). The blue triangles are the simulated PGA values. The difference is that in Fig. 7a), the geometric attenuation function was used where  $R \sim D^2$  (units in cm) for  $D < 30$  km and  $R \sim D$  for  $D \geq 30$  km. In the Fig. 7 b) the function  $R = D$  for all distances was used.

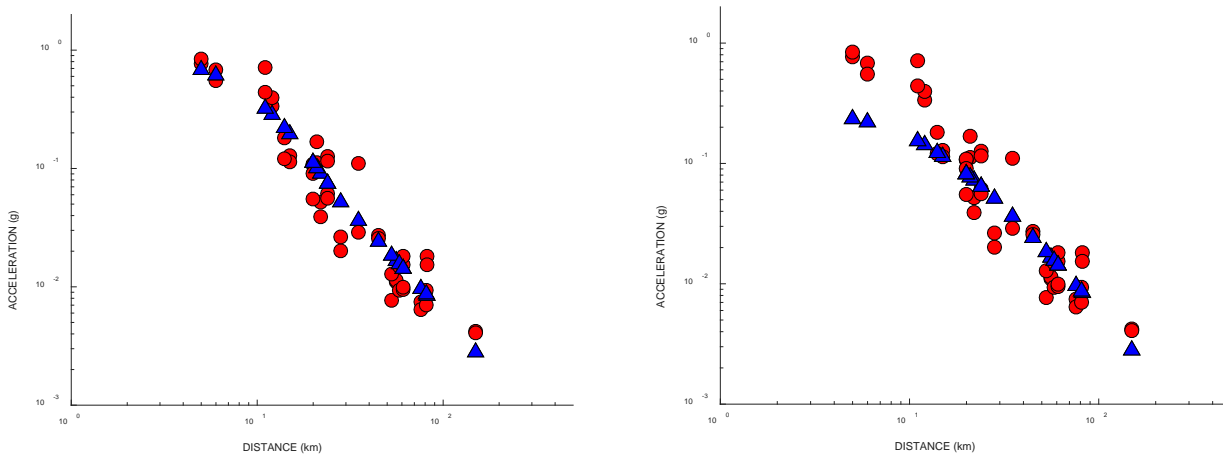


Fig. 7 – PGA values (red dots) and blue triangles are estimated values using Eq. (9) a) With a geometric attenuation function accounting for steeper decay in the near-field b)  $R = D$  for all distances.

## 5. Discussion and conclusions

Source parameters have been obtained for four of the largest earthquake since 1912 in the South Iceland Seismic Zone. A frequency independent  $Q$  and spectral decay parameters that changes slowly with distance. A



representative value of  $\kappa$  for South Iceland is determined to be  $\kappa = 0.045$  s for the area. This is in agreement with the  $\kappa = 0.4$  s - 0.5 s obtained by Ólafsson (1999) from records obtained in lower magnitude earthquakes. The stress drop for the three larger events was found to be approximately 80 bar. The estimated parameters of seismic moment show good agreement with prior studies based on fault plane solutions of distant records [19].

A closed form solution for the calculation of  $a_{rms}$  using the parameters in Brune's point source model is presented in this article. How the parameters obtained from recorded strong-motion acceleration does produce similar values as obtained from the recorded ground motion is demonstrated. It is also demonstrated how it is necessary to account for the high acceleration values close to the source and the rapid attenuation so close to the source, using a geometric attenuation function that gives values similar to those obtained from records. This appears to be a regionally-specific phenomenon and therefore it is necessary to account for this when ground motion is estimated. This is especially important at shorter distances where most of the damage occurs. Possible reasons for these high values are related to the strength of the young volcanic rock resulting in earthquakes with higher stress drops than for example in Californian earthquakes where a stress drop of 50 bar is often used in modelling. The concentration of energy of the fault plane at shallow depths and the faults extending all the way to the top and rupturing the surface could also be contributing factors. In the larger events the rupture surface extends all the way to the top and also down to the base of the crust at a depth of 10 – 15 km.

## 6. Acknowledgements

The research presented herein was supported by the National Power Company and the University of Iceland Research Fund.

## 7. References

- [1] Brune, J.N. (1970). Tectonic stress and the spectra of seismic shear waves from earthquakes. *Journal of Geophysical Research* **75**:26, 4997-5009.
- [2] Hanks, T. C. and McGuire, R. K. (1981), "The character of high-frequency strong ground motion", *Bulletin of the Seismological Society of America* **71**, 2071-2095.
- [3] Boore, J. M. (1983a), "Stochastic simulation of high-frequency ground motions based on seismological models of the radiated spectra", *Bulletin of the Seismological Society of America* **73**, 1865-1894.
- [3] Atkinson, G. M., & Boore, D. M. (1995). Ground-motion relations for eastern North America. *Bulletin of the Seismological Society of America*, **85**(1), 17-30.
- [4] Ólafsson, S., & Sigbjörnsson, R. (1999). A theoretical attenuation model for earthquake-induced ground motion. *Journal of earthquake engineering*, **3** (03), 287-315.
- [5] Ólafsson, S., Sigbjörnsson, R., & Einarsson, P. (1998): Estimation of source parameters and Q from acceleration recorded in the Vatnafjöll Earthquake in South Iceland. *Bulletin of the Seismological Society of America*, **88** (2), 556-563.
- [6] Ólafsson, S. (1999). Estimation of earthquake-induced response. Department of Structural Engineering, Norwegian University of Science and Technology.
- [7] Sigbjörnsson, R., Olafsson, S., Rupakhety, R., Halldorsson, B., Acharya, P., & Snæbjörnsson, J. T. (2014). Strong-motion monitoring and accelerometric recordings in Iceland. In *Proceedings of the second European conference on earthquake engineering*.
- [8] Ólafsson, S., & Sigbjörnsson, R. (2011). Digital filters for simulation of seismic ground motion and structural response. *Journal of Earthquake Engineering*, **15** (8), 1212-1237.
- [9] Ólafsson, S., & Sigbjörnsson, R. (2014): Ground motion prediction equation for south Iceland. *Second European conference on earthquake engineering and seismology*, Istanbul. Turkey.
- [10] Solnes, J., Sigbjörnsson, R., & ELIASSON, J. (2004, August). Probabilistic seismic hazard mapping of Iceland. In *Proceedings of the 13th World conference on earthquake engineering*, Vancouver, BC, Canada.



- [11] N Ambraseys, P Smit, J Douglas, B Margaris, R Sigbjörnsson, S Olafsson (2004): *Bullettino di Geofisica Teorica ed Applicata* **45** (3), 113-129.
- [12] Einarsson, P. (2008). Plate boundaries, rifts and transforms in Iceland. *Jökull*, **58**(12), 35-58
- [13] Ambraseys, N. N., & Sigbjörnsson, R. (2000). *Re-appraisal of the seismicity of Iceland*. publisher not identified.
- [14] Bjarnason, I. T., P. Cowie, M. H. Anders, Seeber, L. and Scholz, C. H. (1993b), "The 1912 Iceland earthquake rupture: Growth and development of a nascent transform system", *Bull. Seism. Soc. Am.* **83**, 416-435.
- [15] Halldorsson, B., & Sigbjörnsson, R. (2009). The Mw6.3 Ölfus earthquake at 15:45 UTC on 29 May 2008 in South Iceland: ICEARRAY strong-motion recordings. *Soil Dynamics and Earthquake Engineering*, **29**(6), 1073-1083.
- [16] Akkar, S., Sandıkkaya, M. A., & Bommer, J. J. (2014). Empirical ground-motion models for point-and extended-source crustal earthquake scenarios in Europe and the Middle East. *Bulletin of earthquake engineering*, **12**(1), 359-387.
- [17] Anderson, J. G., & Hough, S. E. (1984). A model for the shape of the Fourier amplitude spectrum of acceleration at high frequencies. *Bulletin of the Seismological Society of America*, **74**(5), 1969-1993.
- [18] Andrews, D. J. (1986), "Objective determination of source parameters and similarity of earthquakes of different sizes", *Earthquake Source Mechanics*, Maurice Ewing Series 6, Das, S., Boatwright, J. and Sholz, C. H. (editors), *American Geophysical Union, Washington, D. C.*, 259-267.
- [19] Pedersen, R., Jónsson, S., Árnadóttir, T., Sigmundsson, F., & Feigl, K. L. (2003). Fault slip distribution of two June 2000 Mw 6.5 earthquakes in South Iceland estimated from joint inversion of InSAR and GPS measurements. *Earth and Planetary Science Letters*, **213**(3), 487-502.